ISSN 2466-2232 (Print)
ISSN 2466-2100 (Online)

Impact of Wavelengths of CO_2, Disk, and Green Lasers on Fusion Zone Shape in Laser Welding of Steel

Won-Ik Cho*,† and Suck-Joo Na**,***

*BIAS - Bremer Institut für angewandte Strahltechnik GmbH, 28359 Bremen, Germany
**Dept. of Mechanical Engineering, KAIST, Daejeon, 34141, Korea
***School of Materials Science and Engineering, Xi'an Jiaotong University, Xi'an, 710049, China

†Corresponding author : cho@bias.de
(Received May 19, 2020 ; Revised June 10, 2020 ; Accepted June 11, 2020)

Abstract

Numerical simulations of the multi-kW laser welding of structural carbon steel were conducted to analyze the effects of laser wavelength on fusion zone shape. For the heat and mass transfer analysis, the basic governing equations were utilized in addition to the volume-of-fluid (VOF) conservation equation to calculate the free surface boundary. Laser welding models that considered phenomena such as multiple reflections of the laser beam at the keyhole, absorption, recoil pressure, and shear stress and heat source by metal vapor generated were used as well. Two models: a general and a simplified model, which were both based on the Fresnel equations, were considered with the wavelengths of CO_2, disk, and green lasers for calculating of the laser absorptivity of the material. The difference found in the results of the general model and the simplified model in the range of the wavelengths considered, was negligible. In addition, the results obtained for disk laser welding and green laser welding did not exhibit any considerable difference in terms of their impact on the fusion zone shape.

Key Words : Laser welding, Numerical simulation, Laser wavelength, Fresnel reflection model

1. Introduction

Laser welding has the advantage of achieving deep penetration and high welding speed, leaving a relatively low heat affected zone in the weld thanks to its high power density. There are CO_2 lasers and lamp pumped Nd:YAG lasers that are traditionally widely used in the industry. Of them, the CO_2 laser has been widely used in thick plate applications which requires high power, yet has a disadvantage that it cannot be transmitted by optical fiber due to its 10.6 μm wavelength. In contrast, the lamp pumped Nd:YAG laser has been applied to various fields because it can be transmitted by optical fiber. However, it has some shortcomings in that not only its power is limited but the efficiency and quality are deteriorated due to the temperature rise of the laser gain medium, thermal lensing, and depolarization loss. Currently, the application of disk and fiber lasers that overcome these shortcomings is increasing. Since they are able to maintain high efficiency and quality even at high power, they have been widely applied not only in the micro field, but in the thick plate applications mainly covered by the CO_2 laser. Since these lasers operate at a wavelength of approximately 1.03 μm or 1.07 μm, they can be transmitted of course by optical fiber as with the Nd:YAG laser. With the recent increase in the demand for e-mobility, the demand for welding of materials with high electrical conductivity such as copper has also grown. However, these materials have a very low absorptivity for traditional lasers with an infrared wavelength. Thus, application of lasers with a short wavelength (e.g. a green laser with a wavelength of 532 nm) is being examined.

Experimental studies account for the majority of studies on laser welding, but numerical studies have also been actively underway thanks to the advancement of computing technology. Under the assumption that the model used is verified, numerical studies have the advantage of closely observing areas that are difficult to

reach because of experimental constraints. They are of great help in understanding the physical phenomenon of welding. In particular, since the molten pool is formed in fusion welding such as laser welding, molten pool analysis is widely conducted for realistic simulation. With reference to molten pool analysis for laser deep welding, it is crucial to realize the phenomenon that the keyhole is generated by the vaporization of the material due to the high power density (over 10^6 W/cm^2). The simulation of the early laser welding mainly focused on the heat transfer in conduction mode, thus was performed similarly to gas tungsten arc (GTA) welding simulation[1]. Kaplan predicted the 2-dimensional keyhole shape using the energy balance equation considering the multiple reflections and plasma in the laser keyhole. The energy absorbed by multiple reflections was calculated by assuming a conical keyhole. The result showed that the increase in the energy absorbed by multiple reflections had a significant effect on the keyhole shape[2]. The 3-dimensional keyhole shape was also predicted in a similar way[3]. Because it was still hard to predict accurate keyhole shapes, the observed keyhole shape using an X-ray transmission method was also used in laser welding simulation[4]. A study using a predicted keyhole shape to analyze the behavior of the molten pool was also conducted[5]. With the advancement of computing technology and algorithms, numerical simulation of the keyhole shape and the molten pool behavior began to be integrated by applying the level set method and VOF method, which are free surface tracking algorithms[6,7]. Because of the mass conservation error of the level set method and the complex algorithm that attempts to solve it, the VOF-based method is currently widely employed. By extracting the keyhole shape in real-time using the VOF method and applying the ray-tracing technique to the shape, the multiple reflection phenomenon of the laser beam in the keyhole was modeled[8]. Simulation of the laser drilling process taking into account the effect of laser polarization was also performed[9]. As the rapid keyhole change can be calculated in detail in this way, it is possible to simulate the occurrence of pores arising from the collapse of the laser keyhole with a bubble model[10]. It was also simulated how the alloy elements supplied from a filler metal due to the strong flow around the keyhole were distributed on the weld[11]. The path in which the laser beam was focused and diffracted through the laser optics was taken into account, and the effect of the metal vapor generated by the laser was modeled using a shear stress and a heat source. It enabled the prediction of relatively precise results even in a high power laser welding[12]. Recently, a numerical study considering the oscillation of the laser beam was also conducted, and the effect of oscillation frequency on the molten pool was analyzed[13]. In addition, the buttonhole phenomenon arising from the effect of surface tension pressure in laser welding of thin plates was also simulated[14].

In this study, the 3-dimensional computational fluid dynamics (CFD) simulation of laser welding using multi-kW CO_2, disk, and virtual green lasers was performed. The focused and diffracted beam path was used, and the multiple reflections of the beam were considered. The material absorptivity of the laser beam was calculated by the two types of Fresnel reflection models to investigate the effects of laser wavelengths. Buoyancy, Marangoni force, recoil pressure, shear stress and heat source by metal vapor, and bubble model was applied. The final fusion zone shape was used to compare the results.

2. Methodology

Fig. 1 shows the computational domain and mesh for the heat and mass transfer analysis of laser welding. Of the entire domain (56 mm long, 26 mm wide, 15.2 mm high), a fine mesh for the central analysis domain (36 mm long, 6 mm wide, and 15.2 mm high) where the molten pool was formed, and a coarse mesh for the other domain was used. The size of the fine mesh was chosen to be 0.2 mm through a mesh test. The boundary condition on the six sides of the computational domain was defined for the partial derivative value to be 0 (Neumann boundary condition) for all independent variables. In order to perform 3-dimensional transient CFD simulation, the mass conservation equation, momentum equation, and energy conservation equation, which are basic governing equations, were used. Additionally, the VOF equation for free surface tracking was used. Newtonian fluid and incompressible laminar flow were assumed for molten metal. For a laser welding model, the beam path considering the beam focusing phenomenon and diffraction phenomenon by the laser optics was modeled, and multiple reflection phenomenon was simulated using the ray-tracing method. The material absorptivity of the laser beam at the reflected position was determined by the Fresnel reflection model. Along with this, the recoil pressure, Marangoni effect, buoyancy, and shear stress and heat source by metal vapor were considered, and an adiabatic bubble pressure model was applied to investigate the behavior of bubbles generated inside the molten pool caused by the

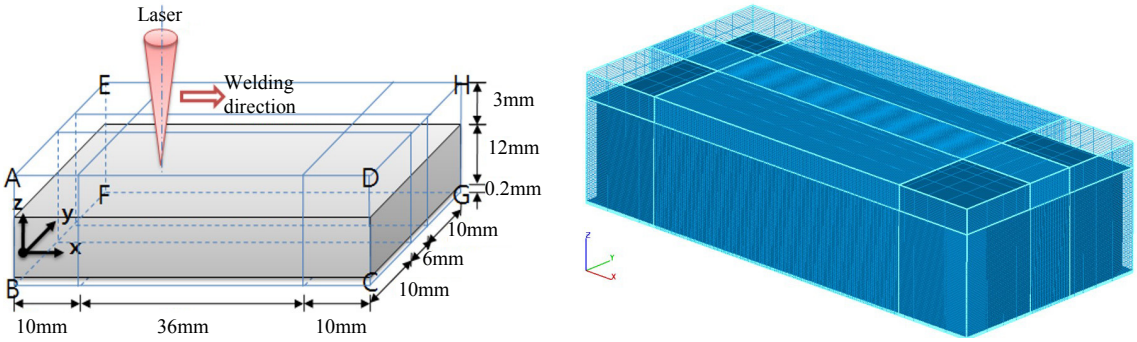

(a) computational domain (b) mesh

Fig. 1 Schematic of the computational domain and mesh for laser welding simulation.

collapse of the keyhole. The literature was referred for the descriptions and formulas for these models and the physical properties of structural carbon steel (A36 (ASTM) or SS400 (JIS)) used for simulation[12].

Two Fresnel models based on the Fresnel equations were used to perform numerical analysis considering different wavelengths of CO_2, disk, and green lasers. Fig. 2 shows the absorptivity data for the laser incidence angle of the general model (based on the Drude theory) and the simplified model (simplified using the Hagen-Rubens relation) (red: general model, blue: simplified model). Table 1 shows the laser and optics parameters used in the simulation. It was assumed that the virtual parameter values for the green laser were the same as the disk laser except for the wavelength and M^2. In all simulation cases, the welding speed was fixed at 1 m/min.

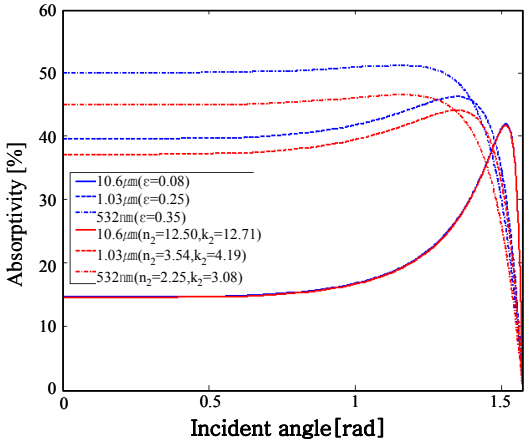

Fig. 2 Absorptivity vs. incident angle based on general and simplified fresnel models for different lasers

3. Results and discussion

Fig. 3 shows the mesh test results. It was found that the calculated penetration depth increased with the decrease in the mesh size, and gradually converged to the keyhole depth of the experimental results. These results are considered to be because in reality the laser beam can reach the bottom of the keyhole as the finer mesh is used. In the simulation, there should be at least an empty space larger than the mesh size in order for the laser beam to pass. Based on the test results, accuracy of simulation can be secured when a mesh size of 0.2 mm or less is used. However, given the calculation time spent, when reducing the mesh size from 0.2 mm to 0.15 mm, it took approximately 2.8 times more time.

Table 1 Laser and optics parameters used

Parameters		CO_2 laser	Disk laser	Green laser
Laser power		4 kW	6 kW	6 kW
Wavelength		10.6 μm	1.03 μm	532 nm
Polarization		Circular	Circular	Circular
Beam quality	M^2	3.8	29.6	57.3
	BPP	12.82 mm·mrad	9.7 mm·mrad	9.7 mm·mrad
Focal length		270 mm	280 mm	280 mm
Beam diameter on optics		33 mm	37 mm	37 mm
Focusing number		8.18	7.5	7.5
Focal radius		209.8	146 μm	146 μm
Rayleigh length		±3.4 mm	±2.2 mm	±2.2 mm
Focal plane		0.0 mm	0.0 mm	0.0 mm

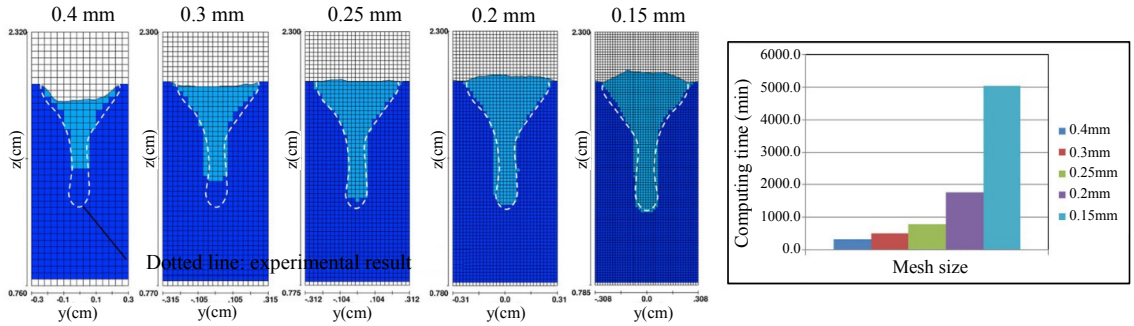

(a) fusion zone shape according to mesh size (b) computing time

Fig. 3 Mesh test in terms of accuracy and efficiency of calculation

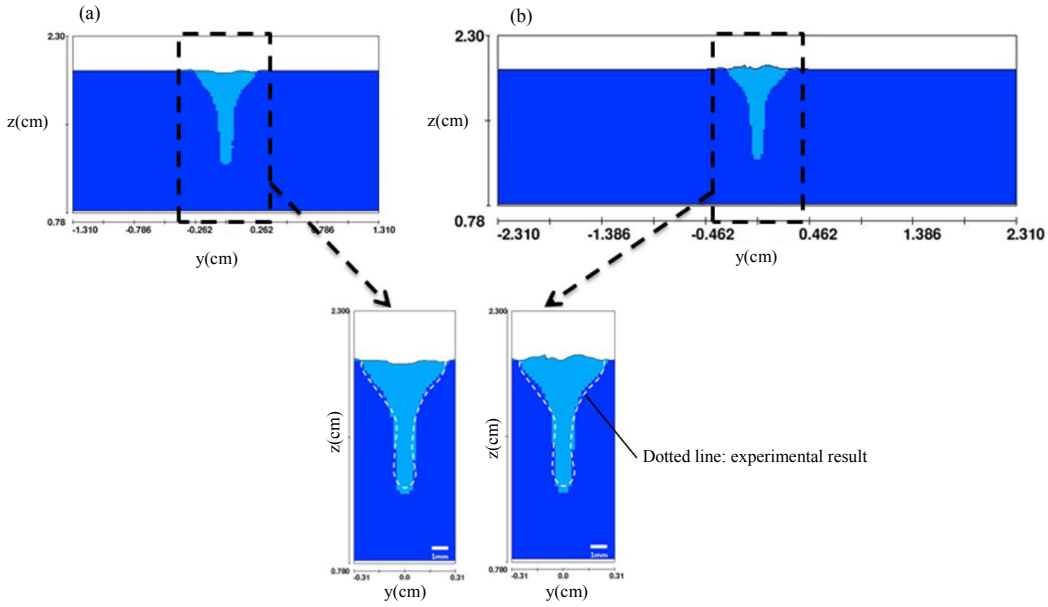

(a) Domain size : 50 mm×26 mm×15.2 mm (b) Domain size : 56 mm×46 mm×15.2 mm

Fig. 4 Fusion zone shapes calculated in different computational domains

Therefore, in this study, a mesh size of 0.2 mm having both accuracy and efficiency was used. The mesh size used in the previous studies on the molten pool behavior of laser welding was different depending on the keyhole depth of the target process. 0.25 mm was used as an optimal value for the shallow keyhole[15], and 0.2 mm for the deep keyhole[16]. This is consistent with the mesh test results of this study. Next, in order to investigate if there was an effect depending on the size of the computational domain, simulation was performed by increasing the width of the computational domain from 26 mm to 46 mm as seen in Fig. 4. The results showed that the predicted differences in fusion zone shapes were negligible, thus the computational domain used in this study was sufficient. As for the computational domain of a width of 26 mm used in this study, the temperature at the boundary showed an increase of approximately 14℃ from the initial temperature during the simulation.

Lastly, the simulation results of the CO_2, disk, and virtual green lasers are shown in Fig. 5. It shows the fusion zone shapes of the YZ cross-section. All of the keyholes grow sufficiently after the start of welding, indicating the result in the steady state. In our previous study, the CO_2 laser and disk laser welding models have already been verified[11,12]. They are considered to be effective even in the range of welding parameters used in this study. The results of applying the two absorption models shown in Fig. 2 were compared. When using the simplified model instead of the general model, the absorptivity has a larger value. In the CO_2 laser wavelength, the two models have almost the same value, yet the difference between them increases with the decrease in wavelength. Despite the difference in the absorptivity between these models, the prediction results of the fusion zone using the two models did not show much difference. In addition, when comparing the results of the disk laser and the green laser, the dif-

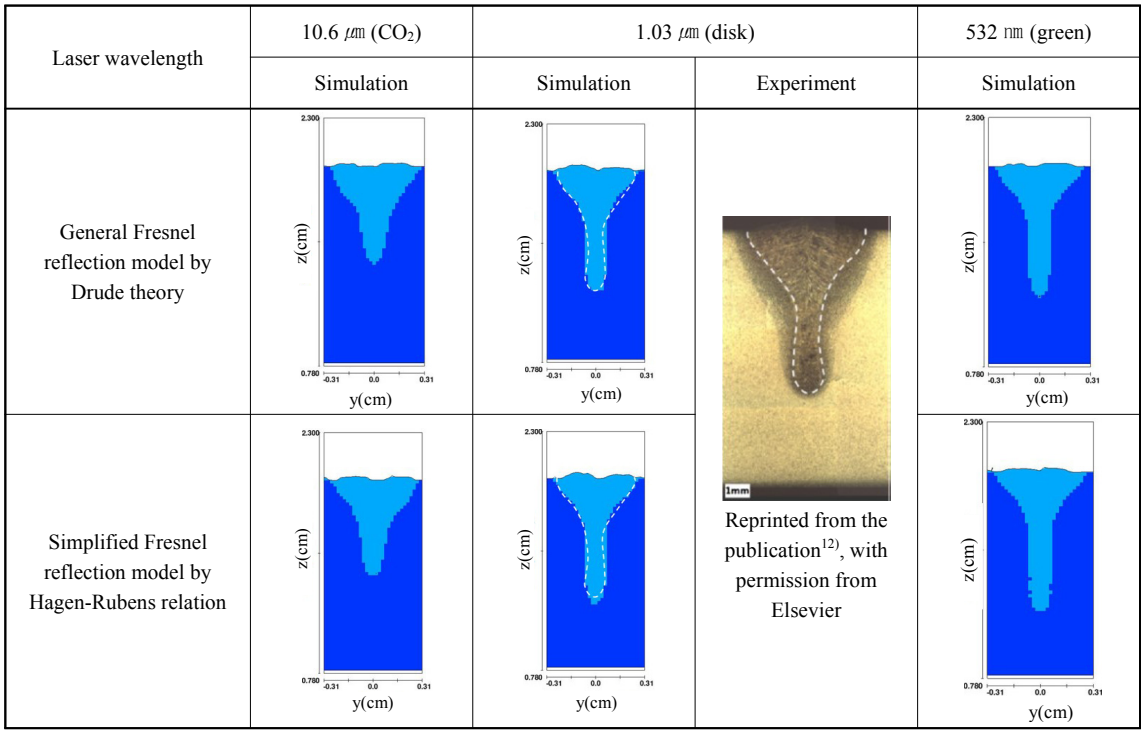

Fig. 5 Fusion zone shapes calculated based on general and simplified Fresnel models for different lasers

ference arising from wavelength changes was also negligible. These results are considered to be because the effect of the models and the wavelengths decreases with the increase in the total absorption (over 80% in this study[12], up to 90% is reported[17]) by the multiple reflection phenomenon for keyhole welding. After the keyhole grew sufficiently, there was no significant change in the fusion zone shapes in the XZ cross-section as well as the YZ cross-section of Fig. 5. These results can also be found in the previous study using the disk laser[12]. However, in the regions where the welding starts and where the welding ends, the depth of the keyhole decreases, thus the difference in the energy absorbed is expected to increase. The difference is also expected to influence the properties of the final weld by affecting the molten pool behavior and the temperature distribution. Especially, since more welding defects are observed in those regions, there is a need for further research in the future.

4. Conclusion

In this study, the numerical simulation considering the wavelengths of CO_2, disk, and green lasers was performed using laser welding models, and the following results were derived.

1) The mesh test showed that the size of 0.2 mm had the accuracy of result and the efficiency of calculation in the range of welding parameters used in this study. Therefore, this mesh size can be recommended for similar laser welding simulations.

2) In terms of the final fusion zone shape, the general model and the simplified model did not show any significant difference. In addition, when comparing the analysis results of the disk laser and the green laser, there was no significant difference even at different wavelengths. This is considered to be because the effect caused by the difference in the models and the wavelengths is negligible due to the significant increase in the total absorption by multiple reflections (80-90%) for the keyhole welding of this study.

Acknowledgement

The authors received no financial support for the research, authorship, and/or publication of this article. This paper contains a part of the contents in the author´s Ph.D. dissertation[18].

ORCID: Won-Ik Cho: https://orcid.org/0000-0002-4047-4230
ORCID: Suck-Joo Na: https://orcid.org/0000-0002-1832-3997

References

1. T. Zacharia, S. A. David, J. M. Vitek and T. Debroy, Weld Pool Development During GTA and Laser Beam Welding of Type 304 Stainless Steel, Part I - Theoretical Analysis, *Weld. J.* 68(12) (1989) 499s-509s.
2. A. Kaplan, A Model of Deep Penetration Laser Welding

Based on Calculation of the Keyhole Profile, *J. Phys. D: Appl. Phys.* 27(9) (1994) 1805-1814.
https://doi.org/10.1088/0022-3727/27/9/002
3. P. Solana and J. L. Ocaña, A Mathematical Model for Penetration Laser Welding as a Free-Boundary Problem, *J. Phys. D: Appl. Phys.* 30(9) (1997) 1300-1313.
https://doi.org/10.1088/0022-3727/30/9/005
4. A. F. H. Kaplan, M. Mizutani, S. Katayama and A. Matsunawa, Unbounded Keyhole Collapse and Bubble Formation During Pulsed Laser Interaction with Liquid Zinc, *J. Phys. D: Appl. Phys.* 35 (2002) 1218-1228.
https://doi.org/10.1088/0022-3727/35/11/319
5. A. Mahrle and J. Schmidt, The Influence of Fluid Flow Phenomena on the Laser Beam Welding Process, *Int. J. Heat Fluid Fl.* 23 (2002) 288-297.
https://doi.org/10.1016/S0142-727X(02)00176-5
6. H. Ki, J. Mazumder and P. S. Mohanty, Modeling of laser keyhole welding: Part I. mathematical modeling, numerical methodology, role of recoil pressure, multiple reflections, and free surface evolution, *Metall. Mater. Trans. A* 33(6) (2002) 1817-1830.
https://doi.org/10.1007/s11661-002-0190-6
7. J. Y. Lee, S. H. Ko, D. F. Farson and C. D. Yoo, Mechanism of keyhole formation and stability in stationary laser welding. *J. Phys. D: Appl. Phys.* 35(13) (2002) 1570-1576.
https://doi.org/10.1088/0022-3727/35/13/320
8. J. H. Cho and S. J. Na, Implementation of Real-Time Multiple Reflection and Fresnel Absorption of Laser Beam in Keyhole, *J. Phys. D: Appl. Phys.* 39 (2006) 5372-5378.
https://doi.org/10.1088/0022-3727/39/24/039
9. J. H. Cho and S. J. Na, Theoretical Analysis of Keyhole Dynamics in Laser Drilling Considering the Polarization of Laser, *J. Phys. D: Appl. Phys.* 40 (2007) 7638-7647.
https://doi.org/10.1088/0022-3727/40/24/007
10. W. I. Cho, J. H. Cho, M. H. Cho, J. B. Lee and S. J. Na, Numerical Simulation of Bubble and Pore Generation by Molten Metal Flow in Laser-GMA Hybrid Welding, *J. Weld. Join.* 26(6) (2008) 67-73.
https://doi.org/10.5781/KWJS.2008.26.6.067
11. W. I. Cho, S. J. Na, M. H. Cho and J. S. Lee, Numerical Study of Alloying Element Distribution in CO_2 Laser-GMA Hybrid Welding, *Comput. Mater. Sci.* 49(4) (2010) 792-800.
https://doi.org/10.1016/j.commatsci.2010.06.025
12. W. I. Cho, S. J. Na, C. Thomy and F. Vollertsen, Numerical simulation of molten pool dynamics in high power disk laser welding, *J. Mater. Process. Technol.* 212 (2012) 262-275.
https://doi.org/10.1016/j.jmatprotec.2011.09.011
13. W. I. Cho, V. Schultz and P. Woizeschke, Numerical study of the effect of the oscillation frequency in buttonhole welding, *J. Mater. Process. Technol.* 261 (2018) 202-212.
https://doi.org/10.1016/j.jmatprotec.2018.05.024
14. W. I. Cho and P. Woizeschke, Analysis of molten pool behavior with buttonhole formation in laser keyhole welding of sheet metal, *Int. J. Heat Mass Trans.* 152 (2020) 119528.
https://doi.org/10.1016/j.ijheatmasstransfer.2020.119528
15. M. H. Cho and D. F. Farson, Simulation Study of a Hybrid Process for the Prevention of Weld Bead Hump Formation. *Weld. J.* 86(9) (2007) 253s-262s.
16. J. H. Cho and S. J. Na, Three-Dimensional Analysis of Molten Pool in GMA-Laser Hybrid Welding, *Weld. J.* 88(2) (2009) 35s-43s.
17. Y. Kawahito, N. Matsumoto, Y. Abe and S. Katayama, Laser absorption characteristics in high-power fibre laser welding of stainless steel, *Weld. Int.* 27(2) (2013) 129-135.
https://doi.org/10.1080/09507116.2011.606151
18. W. I. Cho, Ph. D. dissertation, A Numerical Study on Molten Pool Behavior in Laser-Arc Hybrid Welding Process, *KAIST*, Daejeon, Korea (2012) 48-111.